Influence of Remote Ligand Lone Pairs on the Electronic Structure and Spectrum of Bis(bipyridine)ruthenium(II) 3,4-Diamino-3′,4′-diimino-3′,4′-dihydrobiphenyl. Tuning by External Donors and Acceptors

Robert A. Metcalfe,[†] Elaine S. Dodsworth,[†] Scott S. Fielder,[†] Derk J. Stufkens,[‡] A. B. P. Lever,*[,†] and William J. Pietro[†]

Department of Chemistry, York University, North York, Ontario, Canada M3J 1P3, and Anorganisch Chemisch Laboratorium, J. H. van't Hoff Instituut, Universiteit van Amsterdam, Nieuwe Achtergracht 166, 1018 WV Amsterdam, The Netherlands

Received March 1, 1996[⊗]

The highly solvatochromic title complex comprises a donor diaminobenzene unit (OPDA) linked to an acceptor ruthenium benzoquinonediimine (BQDI) unit. Hydrogen bond donor and acceptor solvents influence the extent to which the amino group lone pairs inject charge into the OPDA ring. The ligand tends toward planarity when the lone pairs conjugate with the OPDA ring and twists when the lone pairs are removed from conjugation by hydrogen bonding to the solvent. The electronic spectra in these two extreme situations are very different due to large changes in the oscillator strengths of certain transitions. Extended Hückel calculations with charge iteration provide a means for calculating these oscillator strengths and for providing a picture of the metal to ligand and internal OPDA to BQDI charge transfer which occurs. A ZINDO/1 geometry optimization provides additional evidence for the model developed.

1. Introduction

The complex[1] $[Ru(bpy)_2(dadib)](PF_6)_2$, **1**, where dadib = 3,4-diamino-3′,4′-diimino-3′,4′-dihydrobiphenyl and bpy = 2,2′-bipyridine, is relevant to a number of areas of current inorganic research. It has no center of symmetry and comprises an

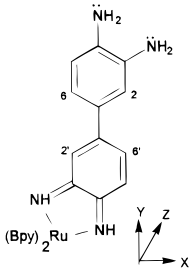

1

electron donor and an electron acceptor fragment and as such fits most of the criteria for a molecule having nonlinear optical properties such as second harmonic generation,[2−6] and is of interest with respect to the use of a twist angle to control electron transfer between donor and acceptor, e.g., refs 7−9 (and references cited therein). It is also pertinent to molecular wire research being capable of forming strongly coupled bridging systems, e.g., refs 10−14.

This paper describes how solvent can control the coupling or uncoupling of the two remote lone pairs on the 3- and 4-amino groups with the ruthenium benzoquinonediimine (BQDI) moiety causing a dramatic change in the electronic spectrum; in effect the solvent switches on or off the donor−acceptor interaction between the remote amino groups and the metal.

Complex **1**, in certain solvents, has two intense electronic transitions in the visible region involving several metal d orbitals and the dadib ligand. This observation is at variance with previous work of this group[15,16] on the closely related BQDI complexes, which have only one intense transition in the visible region, and one very weak transition, in the near-infrared (near-IR), involving the metal d orbitals and the BQDI ligand.

In the dadib system, the energies and intensities of these two transitions were found to be highly dependent upon the solvent

[†] York University.
[‡] Universiteit van Amsterdam.
[⊗] Abstract published in *Advance ACS Abstracts*, December 1, 1996.

(1) Metcalfe, R. A.; Dodsworth, E. S.; Lever, A. B. P.; Pietro, W. J.; Stufkens, D. J. *Inorg. Chem.* **1993**, *32*, 3581.
(2) Eaton, D. F.; Meredith, G. R.; Miller, J. S. *Adv. Mater.* **1991**, *3*, 564. Eaton, D. F.; Meredith, G. R.; Miller, J. S. *Adv. Mater.* **1992,** *4*, 45.
(3) Williams, D. J. *Angew. Chem., Int. Ed. Eng.* **1984**, *23*, 690.
(4) Nalwa, H. S. *Appl. Organomet. Chem.* **1991**, *5*, 349.
(5) Tam, W.; Cheng, L. T.; Bierlein, J. D.; Cheng, L. k.; Wang, Y.; Feiring, A. E.; Meredith, G. R.; Eaton, D. F.; Calabrese, J. *ACS Symp. Ser.* **1991**, *455*, 158.
(6) Takagi, K.; Ozaki, M.; Nakatsu, K.; Matsuoka, M.; Kitao, T. *Chem. Lett.* **1989**, 173.
(7) Launay, J. P.; Joachim, C. *J. Chim. Phys.* **1988**, *85*, 1135.
(8) Woitellier, S.; Launay, J. P.; Joachim, C. *Chem. Phys.* **1989**, *131*, 481.
(9) Lewis, N. *Inorg. Chem.* **1995**, *34*, 2244.
(10) Bignozzi, C. A.; Argazzi, R.; Schoonover, J. R.; Gordon, K. C.; Dyer, R. B.; Scandola, F. *Inorg. Chem*, **1992**, *31*, 5260. Creutz, C.; Newton, M. D.; Sutin, N. *J. Photochem. Photobiol. A. Chem.* **1994**, *82*, 47. Haga, M.; Ano, T.; Ishizaki, T.; Kano, K.; Nozaki, K.; Ohno, T. *J. Chem. Soc., Dalton Trans.* **1994**, *263*. Rezvani, A. R.; Evans, C. E. B.; Crutchley, R. J. *Inorg. Chem.* **1995**, *34*, 4600.
(11) Bolger, J.; Gourdon, A.; Ishow, E.; Launay, J. P. *J. Chem. Soc., Chem. Commun.* **1995**, 1799, Salaymeh, F.; Berhane, S.; Yusof, R.; de la Rosa, R.; Fung, E. Y.; Matamoros, R.; Lau, K. W.; Zheng, Q.; Kober, E. M.; Curtis, J. C. *Inorg. Chem.* **1993**, *32*, 3895, Lewis, N. A.; Pan, W. *Inorg. Chem.* **1995**, *34*, 2244.
(12) Ribou, A.-C.; Launay, J. P.; Takahashi, K.; Takayasu, N.; Tarutani, S.; Spangler, C. W. *Inorg. Chem.* **1994**, *33*, 1325. Watzky, M. A.; Song, X. Q.; Endicott, J. F. *Inorg. Chim. Acta* **1994**, *226*, 109.
(13) Beley. M.; Collin, J.-P.; Louis, R.; Metz, B.; Sauvage, J.-P. *J. Am. Chem. Soc.* **1991**, *113*, 8521. Ferretti, A.; Lami, A.; Ondrechen, M. J.; Villani, G. *J. Phys. Chem.* **1995**, *99*, 10484. Scandola, F.; Argazzi, R.; Bignozzi, C. A.; Chiorboli, C.; Indelli, M. T.; Rampi, M. A. *Coord. Chem. Rev.* **1993**, *125*, 283.
(14) Auburn, P. R.; Lever, A. B. P. *Inorg. Chem.* **1990**, *29*, 2551.
(15) Masui, H.; Lever, A. B. P.; Auburn, P. R. *Inorg. Chem.* **1991**, *30*, 2402.
(16) Masui, H.; Dodsworth, E. S.; Lever, A. B. P. *Inorg. Chem.* **1993**, *32*, 258.

S0020-1669(96)00232-7 CCC: $12.00

in which **1** was dissolved. It was further demonstrated[1] by AM1 semiempirical calculations on a model complex[17] $[F_2B(dadib)]^+$ that the dihedral angle between the two six-membered rings of the dadib ligand changes as a consequence of the interaction of the two terminal amino groups of the dadib ligand with hydrogen bond donors (electron acceptors) and hydrogen bond acceptors (electron donors). The previous calculations showed that the free $[F_2B(dadib)]^+$ complex in the gas phase had a dihedral angle between the two six-membered rings of 25.5°. For the dadib ligand the two competing forces which determine the size of the dihedral angle between the two rings are the unfavorable interaction between 2,2′ and 6′,6 hydrogen atoms, causing the dihedral angle to increase, and the favorable electronic interaction between the electron rich *o*-phenylenediamine (OPDA) ring and the electron deficient BQDI ring which will cause the dihedral angle to decrease. Interaction with electron donors was found to enrich the electron density on the amino groups, thus favoring lone pair donation into the OPDA ring. The electron rich OPDA ring then donates some of its π density to the benzoquinonediimine ring. The favorable donor−acceptor interaction overcomes some of the steric repulsion of the 2′,6 and 6′,2 hydrogen atoms and drives the dihedral angle to decrease, simultaneously shortening the C−C bridge between the two six-membered rings; i.e., this bridge takes on some double bond character.

Conversely, competition for the lone pairs of the amino groups by hydrogen bond donors (electron acceptors) diminishes the electron density on the OPDA ring. This results in the loss of the favorable donor−acceptor interaction between the two rings, and, as a result, the steric repulsion prevails[18] and the dihedral angle between the two rings increases.

In summary, in the hydrogen bond donor solvent water, the dihedral angle tends to twist towards 90°, while, in the hydrogen bond acceptor solvent dimethyl sulfoxide (DMSO), the twist angle approaches zero, i.e., coplanarity of the two rings. The controlling mechanism for the change in the twist angle is demonstrated here to be the involvement of the $-NH_2$ lone pairs in the π system of the ligand. We show by more detailed assignment of the electronic spectrum and, in particular, analysis of the variations in the oscillator strengths of the pertinent electronic transitions that the detailed spectroscopic changes (solvatochromism) can be understood in terms of this mechanism. In the previous paper,[1] greater emphasis was placed upon the change in the twist angle at the 1,1′-C,C bridge; here, we will demonstrate that this change in twist angle is concomitant with the more fundamental change in donor−acceptor coupling between the amino group lone pairs and the distant ruthenium BQDI fragment.

Unfortunately this system shows no luminescence, and hence excited state quenching information, which might have provided a direct measurement of electron transfer rates between the donor and acceptor.

2. Experimental Section

The complex $[Ru(bpy)_2(dadib)]^{2+}$ was synthesized according to a published procedure[14] and isolated as either a PF_6^- or BF_4^- salt. All solvents that were used were reagent grade or better and were purified according to literature procedures.[19] Water was purified by distillation from $KMnO_4$, followed by passage through a Barnstead organic removal cartridge and two Barnstead mixed-resin Ultrapure cartridges.

The pH measurements were made using a Fisher Accumet Model 120 pH meter, with an Aldrich pH combination electrode. The pH electrode was submerged in a 2.1×10^{-5} M aqueous solution of the $[Ru(bpy)_2(dadib)]^{2+}$ complex. The solution was titrated with microliter amounts of concentrated or 1% HCl and 10 M or 0.1 M NaOH which were added via microliter syringes. The spectroscopic changes were recorded, and the pK_a was determined using the relationship[20]

$$pK_a = pH + \log(A_I - A)/(A - A_M) \quad (1)$$

where A_I is the absorbance of the protonated species, A is the absorbance of a mixture, and A_M is the absorbance of the nonprotonated species.

Boron trifluoride etherate was purified according to a literature procedure.[19] It was diluted to 0.08 M by addition of dry diethyl ether. The BF_3 was added by microliter syringe to a 6.93×10^{-5} M solution of the $[Ru(bpy)_2(dadib)](PF_6)_2$ complex in 1,2-dichloroethane, and the spectroscopic changes were recorded.

Cyclic voltammograms were obtained using Princeton Applied Research Corp. Models 173, 174, and 179 instrumentation or using a Pine Instruments RDE-3 potentiostat. Platinum wires were used as the working and counter electrodes. Solutions typically contained 0.1 M $(TBA)PF_6$. A silver chloride-coated silver wire, separated from the bulk solution by a frit, served as a quasi reference electrode. Ferrocene was added to all solutions as an internal standard (0.425 V vs SCE in acetonitrile).[21]

Electronic spectra were measured using a Varian-Cary Model 2400 UV−vis−near-IR spectrophotometer. Spectra were deconvoluted into Gaussians using an in-house basic program. Oscillator strengths were calculated by first using the deconvolution program to break the spectrum down into a series of Gaussians and then using the formula

$$f \approx 4.6 \times 10^{-9} \epsilon_{max} \Delta_{1/2} \quad (2)$$

where ϵ_{max} is the molar intensity of the Gaussian and $\Delta_{1/2}$ is its half-bandwidth. The solid state spectrum of species **1** was recorded as a Nujol mull using a Guided Wave Inc. optical waveguide spectrometer, Model 100.

Molecular orbital calculations were performed at the Extended Hückel level (EHMO) using in-house code,[22] with charge iteration (EHMO-CIT)[23] and Ru bases from ref 24. The EHMO-CIT calculations were ported to the Spartan program (Wavefunction Inc., Irvine, CA). Data were processed on a Silicon Graphics Personal Iris Indigo R4000 or IBM350 RISC 6000 computer.

Molecules were assembled in the Spartan 3.0 Builder. The Ru−N (dadib) bond distances were constrained to be[25] 2.02 Å, and the dihedral angles between the two six-membered rings, 0−45° as desired. The amino groups were constrained to have their lone pairs either in the π system or perpendicular to the π system of the OPDA ring. The conformation in which the 3-amino group is trans to the 3′-imino group was used. The constrained structures were then minimized within the Spartan Builder and submitted to the EHMO-CIT program.

Oscillator strengths were generated using extended Hückel wave functions developed following the method of Calzaferri[26] but with some variations and using in-house code.[27]

Resonance Raman data were collected using a Dilor *XY* spectrometer using an SP 2016 argon laser, and a CR 590 dye laser with rhodamine 6G and coumarin 6 as dyes, as the excitation source. Data were collected using a spinning cell with either water or DMSO as the solvent. The Raman spectra were obtained by excitation with 457.9, 488, 514.5, 568, 587, and 619 nm in water and with 457.9, 488, 514.5, 531, 550, 569, 586, 606, and 622 nm in DMSO. The 1050 cm^{-1} Raman

(17) In the absence of AM1 basis sets for ruthenium, a $[BF_2]^+$ unit was used to simulate that moiety; the compound itself has not been prepared.

(18) Adamo, J. *Chem. Phys. Lett.* **1974**, *6*, 135.
(19) Perrin, D. D.; Armarego, W. L. F.; Perrin, D. R. *Purification of Laboratory Chemicals*, 2nd ed.; Pergamon Press: Elmsford, New York, 1980.
(20) Albert, A.; Serjeant, E. P. "*The Determination of Ionization Constants*", Chapman and Hall Ltd., London, **1971**.
(21) Gennett, T.; Milner, D. F.; Weaver, M. J. *J. Phys. Chem.* **1985**, *89*, 2787.
(22) Hoffman, R. J. *Chem. Phys.* **1963**, *39*, 1397.
(23) Basch, H.; Viste, A.; Gray, H. B. *J. Chem. Phys.* **1966**, *44*, 10.
(24) Vela, A.; Gazquez, J. L. *J. Phys. Chem.* **1988**, *92*, 5688.
(25) Belser, P.; von Zelewsky, A.; Zehnder, M. *Inorg. Chem.* **1981**, *20*, 3098.
(26) Calzaferri, G.; Rytz, R. *J. Phys. Chem.* **1995**, *99*, 12141.
(27) Fielder, S. S.; Lever, A. B. P.; Pietro, W. J. Work in progress.

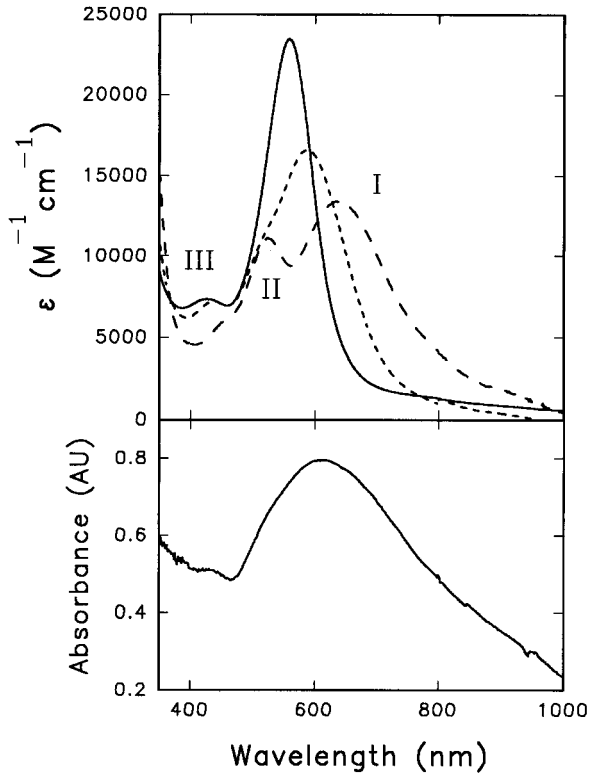

Figure 1. Electronic spectrum of $[Ru(bpy)_2(dadib)](PF_6)_2$ in water (solid line), acetonitrile (···), DMSO (- -), and (lower panel) solid state mull absorbance.

band of potassium nitrate was used as an internal standard when the solvent was water, and DMSO vibrations were used when the solvent was DMSO. Excitation profiles were plotted by measuring the height of the enhanced vibration and then dividing that by the height of the internal standard. Since the internal standards have no low-energy electronic transitions, the Raman intensities of their vibrations follow the normal ν^4 dependence on the frequency of the exciting line. The resonance enhanced vibrations of the complex show, however, an additional dependence of their Raman intensities on the frequency difference between the allowed electronic transition and the exciting laser line.

3. Results and Discussion

3.1. Resonance Raman Spectroscopy.[28] Figure 1 shows the electronic spectrum of complex **1** in water, acetonitrile, DMSO, and the solid state. The visible region is dominated by two or three (depending on solvent) intense electronic transitions, bands I, II, and III.[1] There are also shoulders in the near-IR spectra which are discussed below.

Band III has been assigned[1,14−16] as a Ru d → π*(bpy) metal to ligand charge transfer (MLCT) transition and rR excitation into this band shows enhancement of bipyridine skeletal vibrations[29−31] at 1177, 1318, 1493, 1564, and 1600 cm^{-1}, confirming this assignment.

Excitation of the complex in DMSO (Figure 2) gives rise to different rR effects for excitation into band I and band II. Upon excitation into band I a rR effect is observed for a band at 575 cm^{-1}, believed to be largely Ru−N (vibration of the $Ru(NH)_2$ metallocycle), and for dadib vibrations at 1250, 1360, and 1470

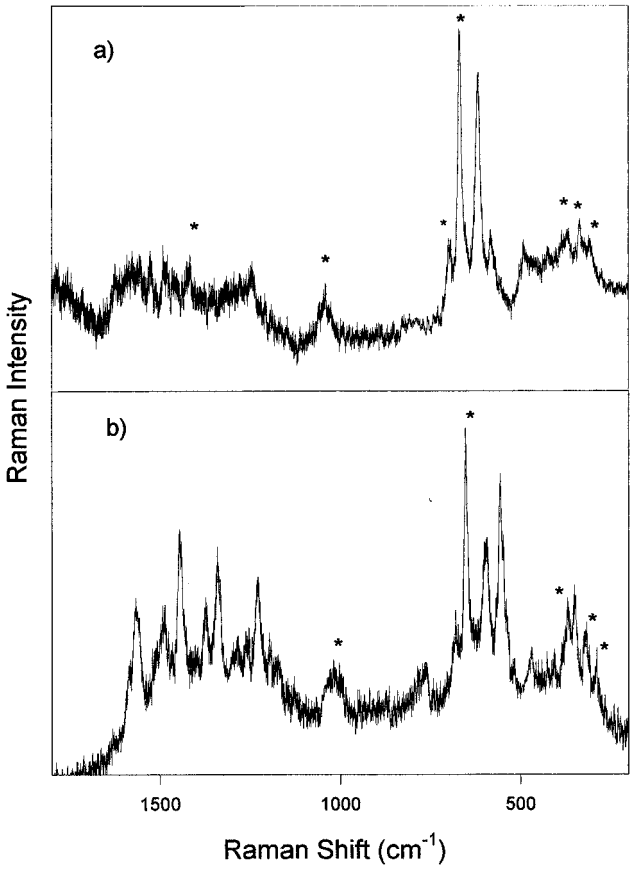

Figure 2. Resonance Raman spectra of $[Ru(bpy)_2(dadib)](PF_6)_2$ dissolved in DMSO. Excitation wavelengths are (a) 488 nm, enhanced vibration at 620 cm^{-1}, and (b) 622 nm. Enhanced vibrations at 1580, 1510, 1470, 1395, 1370, 1250, 610, and 570 cm^{-1}. Vibrations marked with an asterisk derive from DMSO.

cm^{-1}. According to these rR spectra, band I will belong to at least one Ru d → π*(dadib) transition. On excitation into band II the dadib vibrations are no longer enhanced as clearly observed in the excitation profiles shown in Figure 3. The disappearance of ligand vibrations has been noted before for many diimine complexes.[16,29,32,33] This effect is encountered when a metal d orbital strongly mixes with the π* orbital to which the electronic transitions are directed. The electronic transition between these orbitals has relatively little charge transfer character and is, instead, metal−ligand bonding to metal−ligand antibonding. The ligand bonds are largely unaffected by such a transition, thereby explaining the absence of an rR effect for any dadib vibrations.

Concomitant with the disappearance of the dadib vibrations upon excitation into band II is the appearance of a new Ru−N vibration (another vibration of the $Ru(NH)_2$ metallocycle),[34] at 618 cm^{-1} at the expense of the 575 cm^{-1} band. Apparently, the MLCT transition of band I affects only one of the Ru−N bonds, the other being mainly affected by the corresponding transition of band II.

rR spectra of complexes possessing MLCT transitions to inherently asymmetric ligands have been reported before,[35−37]

(28) Clark, R. J. H. *NATO ASI Ser., Ser. C* **1989**, *288*, 301. Clark, R. J. H.; Stewart, B. *Struct. Bonding* (*Berlin*) **1979**, *36*, 1.
(29) (a) Hage, R.; Haasnoot, J. G.; Stufkens, D. J.; Snoeck, Th. L.; Vos, J. G.; Reedijk, J. *Inorg. Chem.* **1989**, *28*, 1413. (b) Stufkens, D. J.; Snoeck, Th. L.; Lever, A. B. P. *Inorg. Chem.* **1988**, *27*, 953.
(30) Mallick, P. K.; Danzer, G. D.; Strommen, D. P.; Kincaid, J. *J. Phys. Chem.* **1988**, *92*, 5628.
(31) Berger, R. M.; McMillen, D. R. *Inorg. Chim. Acta* **1990**, *177*, 65.
(32) Balk, R. W.; Stufkens, D. J.; Oskam, A. *J. Chem. Soc., Dalton Trans.* **1982**, 275.
(33) Stufkens, D. J. *Coord. Chem. Rev.* **1990**, *104*, 39.
(34) These two vibrations are probably better ascribed as symmetric and antisymmetric vibrations of the $Ru(NH)_2$ metallocycle. However, it is probable that in the effective C_1 symmetry they are partially localized on individual Ru−N bonds.
(35) Lever, A. B. P.; Masui, H.; Metcalfe, R. A.; Stufkens, D. J.; Dodsworth, E. S.; Auburn, P. R. *Coord. Chem. Rev.* **1993**, *125*, 317.

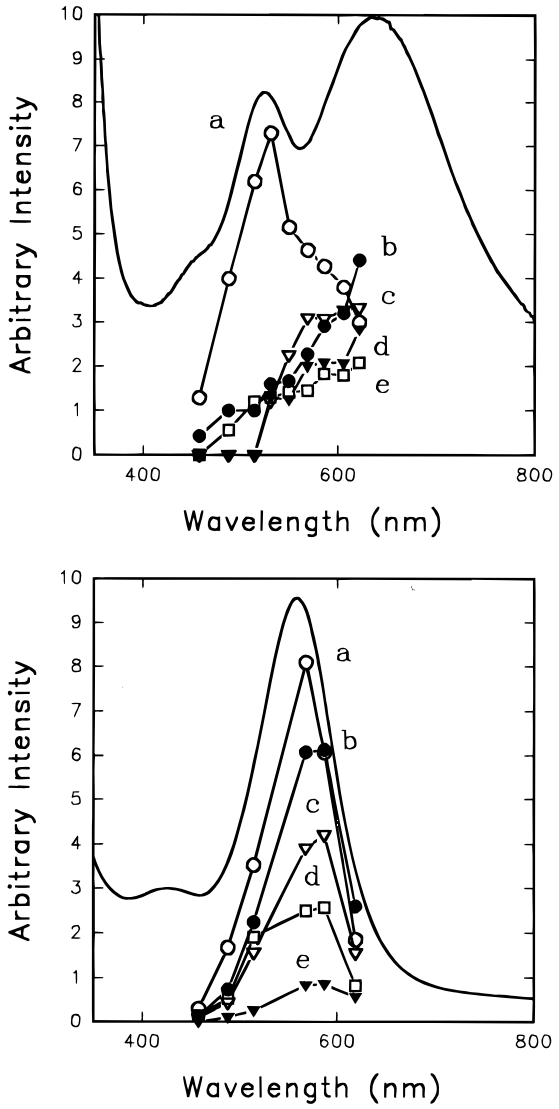

Figure 3. Upper: Excitation profiles of the resonance Raman enhanced vibrations of $[Ru(bpy)_2(dadib)](PF_6)_2$ in DMSO. The vibrations are (a) 618, (b) 575, (c) 1470, (d) 1360, and (e) 1250 cm^{-1}. Lower: Excitation profiles of the resonance Raman enhanced vibrations of $[Ru(bpy)_2(dadib)](PF_6)_2$ in water. The vibrations are (a) 618, (b) 575, (c) 1470, (d) 1250, and (e) 1360 cm^{-1}.

but, to our knowledge, the influence of this symmetry on the rR effects of the metal−ligand stretching vibrations has only been observed in the case[35] of $[Ru(bpy)_2((NO)qH)]^{2+}$. This complex ion contains the asymmetric ligand (NO)qH which represents *o*-aminophenol in its quinonoid oxidation state. Also in this case the rR spectra show the presence of two Ru−(NO)-qH stretching vibrations at 548 and 598 cm^{-1}, which behave differently upon changing the wavelength of excitation.

The interpretation in the case of the aqueous solution data is less certain, but the data are consistent with the presence of both bands I and II lying under the band envelope (Figure 3). Thus band I, which is at lower energy and separated from band II in DMSO, has moved close to band II in aqueous solution.

The excitation profiles reveal that bands I and II are each uniquely associated with each of the two different ruthenium−metallocycle vibrations and that the two transitions which are clearly visible in DMSO solution overlap in aqueous solution.

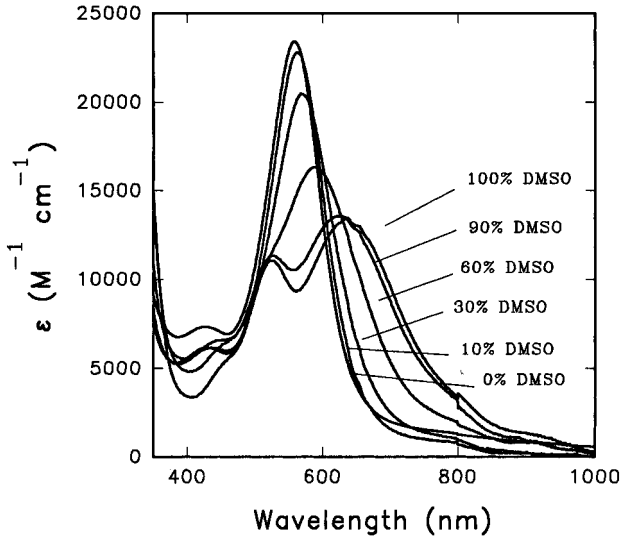

Figure 4. Spectroscopic changes that occur when $[Ru(bpy)_2(dadib)](PF_6)_2$ is dissolved in mixtures of water and DMSO with relative concentrations as noted.

This apparently differs from the situation with the BQDI complexes which have only one Ru−N metallocycle vibration, i.e., the Ru−N bonds are equivalent and only one intense, visible region transition (and a very weak lower energy satellite);[15,16] as will be seen below, however, the BQDI and dadib systems are closely related.

3.2. Solvatochromism. While band II is not appreciably solvatochromic, band I, which we demonstrate later, has some MLCT character, is, like many other charge transfer bands,[38] highly solvatochromic and overlaps band II in certain solvents (Figure 1) and solvent mixtures (Figure 4). Band II frequently appears as a high-energy shoulder of imprecise energy, due to overlap with band I (e.g., Figure 1, acetonitrile). Band III is also solvatochromic. The solvatochromic shifts of bands I and III do not correlate with the Gutmann donor or acceptor number,[39] the Kosower *Z* scale,[40] or the Reichardt E_T[41] parameter, nor do they correlate with McRae's[42] equation. However, their energies correlate reasonably well with a two parameter fit of the Taft and Kamlet hydrogen bond donor (α) and hydrogen bond acceptor (β) parameters as reported previously,[43,44] (see eqs 3 and 4 and Table 1). Three parameter fits were explored but offered no additional insights or improvements. The correlation (Figure 5, upper) between α and β and the energy of band I is given by

$$E[\text{band I}]/\text{cm}^{-1} = [(-2180 \pm 290)\beta + (1040 \pm 140)\alpha + (17400 \pm 160)] \qquad R = 0.94;\ 12\ \text{solvents} \quad (3)$$

where the numbers in parentheses are the standard errors as calculated by the Lotus 123 regression procedure. At the extreme ends of the correlation (Figure 5, upper) are DMSO and methanol. With increasing α contribution band I shifts to the blue, and with increasing β contribution the energy of band I shifts to the red. Water, which had previously been included[1] in the plot for band I, is omitted here because in water band I

(36) Danzer, G. D.; Golus, J.; Kincaid, J. R. *J. Am. Chem. Soc*. **1993**, *115*, 8643.
(37) Treffert-Ziemelis, S. M.; Golus, J. A.; Kincaid, J. R. *Inorg. Chem*. **1993**, *32*, 3890.
(38) Lever, A. B. P. *Inorganic Electronic Spectroscopy*, 2nd ed.; Elsevier Science Publishers: Amsterdam, 1984.
(39) Gutmann, V. *The Donor-Acceptor Approach to Molecular Interactions*; Plenum Press: New York, 1980.
(40) Kosower, E. M. *J. Am. Chem. Soc.* **1958**, *80*, 3253.
(41) Reichardt, C. *Angew. Chem., Int. Ed. Engl*. **1965**, *4*, 29.
(42) McRae, E. G. *J. Phys. Chem*. **1957**, *61*, 562.
(43) Kamlet, M. J.; Abboud, J. L.; Abraham, R. W.; Taft, R. W. *J. Org. Chem*. **1983**, *48*, 2877.
(44) Hansch, C.; Leo, A.; Taft, R. W. *Chem. Rev.* **1991**, *91*, 165.

Table 1. Energies (cm^{-1}) of Bands I−III for the Complex $[Ru(bpy)_2(dadib)](PF_6)_2$ in Different Solvents (log ϵ in Parentheses)

solvent	band I	band II	band III	β	α	$Ru^{III/IIa}$
water		17 890 (4.37)	23 560	0.18	1.1	1.41
water/H^+ [b]		18 480	23 620			
MeOH	16 950	19 540 sh	22 595	0.62	0.93	1.23
CH_3CN	16 895 (4.22)	19 480 (4.11) sh	22 910	0.31	0.19	1.29
prop carb [c]	16 700 (4.23)	19 190 (4.06) sh	22 690	0.40	0.0	1.25
DCE	16 940	19 400 sh	22 450	0.0	0.3	1.20
acetone	16 575	19 150 sh	22 760 sh	0.48	0.08	1.26
EtOH	16 450	19 200 sh	22 430 sh	0.77	0.83	1.20
2-propanol	16 340	19 010 sh	22 330 sh	0.95	0.76	1.18
BuOH	16 300	19 070 sh	22 400 sh	0.88	0.79	1.20
butanone	16 290 (4.19)	19 040 (4.08)	22 260 sh	0.48	0.06	1.17
THF	16 120	19 120	22 390 sh	0.55	0.0	1.19
DMF	16 040 (4.16)	19 065 (4.08)	22 250 sh	0.69	0.0	1.17
DMSO	15 750 (4.14)	19 060 (4.07)	22 090 sh	0.76	0.0	1.14
BF_3/DCE [d]		18 150	23 640			
DMA	15 470	19 115	22 090 sh	0.76	0.0	1.14
solid	16 290	19 050 sh	23 260 sh			1.36

[a] Calculated $Ru^{III/II}$ potential vs SCE, in volts, using eq 5.[50] [b] pH 1.05. [c] Propylene carbonate. [d] 1:1 mixture of species **1** and BF_3.

is too weak for its position to be identified (see below). Previously we had assumed band I was coincident with band II, but this is not assured.

The correlation (Figure 5, lower) between α and β and the energy of band III is given by the following relationship:

$$E[\text{band III}]/\text{cm}^{-1} = [(-1430 \pm 175)\beta + (480 \pm 90)\alpha + (23200 \pm 140)] \qquad R = 0.95;\ 13\ \text{solvents} \quad (4)$$

Band III is less sensitive to the effect of the solvent than is band I, but it too shifts to the blue with increasing α value and to the red with increasing β value.

3.2.1. Mixed Solvent Studies. The resonance Raman spectra suggest that band I remains on the low-energy side of band II, even in aqueous solution, and this can be verified by following the changes in the electronic spectrum of **1** when it is dissolved in solvent mixtures of water and DMSO. Figure 4 shows the changes in the electronic spectrum of **1** as a function of the percentage of water in solution, indicating that as the percentage of water is increased, band I moves closer to band II, producing a spectrum that is similar to the spectrum in acetonitrile solution when the solution is 60% DMSO, until finally producing the spectrum in aqueous solution. Thus, it is likely that band I remains on the low-energy side of band II in all solvents; i.e., bands I and II have not crossed. As the percentage of water is increased, band I shifts to the blue, while the energy of band II is essentially unchanged as the solvent is changed from DMSO to water. There is, however, an apparent increase in intensity in band II and a decrease in intensity of band I as it draws closer.

3.2.2. Oscillator Strengths. Experimental oscillator strengths were derived from the total area covered by bands I and II in DMSO, water, acetonitrile, and the DMSO/water solvent mixtures, at the different pH's and with different amounts of BF_3 added. The results varied between $f \approx 0.32$ and $f \approx 0.37$; thus, the overall probability of bands I and II varies little in these experiments, in spite of the changes in the appearance of the spectrum, and the position of the bands. The intensity apparently lost from band I moving from pure DMSO to pure water (Figure 4) appears to be transferred to band II.

3.2.3. Low-Energy Shoulders. There are low-energy shoulders which appear in the region 10 000−12 500 cm^{-1} in all spectra, though they appear most intense in DMSO (Figures 1, 5, and 7). Addition of BF_3 to a 1,2-dichloroethane solution of **1** or protonation in aqueous medium (see below) causes the low-energy features to appear to weaken, and apparently shift to the blue, but a tail on the low-energy side of band I remains; see Figure 6 (lower). We return to these features below.

3.3. Lewis Acid Equilibria. Hydrogen bond donor solvents can hydrogen bond to the lone pairs of the amino groups of complex **1**. Lewis acids will have little to no interaction with the imino protons but will actually bind directly to the lone pairs of the amino groups. Figure 6 (upper) shows the spectroscopic changes that occur when **1** becomes protonated. As acid is added to an aqueous solution of **1**, the single band shifts to higher energy and becomes more intense. The pK_a of the monoprotonated form was determined spectrophotometrically to be 3.4. The pK_a of the monoprotonated free ligand (3,3′,4,4′-tetraaminobiphenyl) has been determined electrochemically in dimethylformamide (DMF)[45] to be 6.2. The 3 orders of magnitude difference in K_a between the free ligand and the complex can be attributed to the electron withdrawing effect of the $[Ru(bpy)_2]^{2+}$ fragment and the oxidation of part of the ligand to the diimine form, both of which will greatly reduce the electron density on the amino groups. There was no evidence for the second protonation step for dadib in the pH region from 1.6 to 0.5.

Figure 6 (lower) shows the spectroscopic changes that occur when 1 equiv of BF_3 is added to a 1,2-dichloroethane solution of complex **1**. The spectrum initially is similar to that of **1** dissolved in acetonitrile, with bands I−III and a low-energy shoulder clearly visible. However, as BF_3 is added bands I and II coalesce. Eventually, as 1 full equiv of BF_3 is added, the spectrum becomes very similar to the spectrum of **1** dissolved in water.

3.4. Electrochemistry. In acetonitrile solution **1** has two reversible reduction waves,[1] at −0.51 and −1.13 V vs SCE, (−0.54 and −1.09 V vs SCE in DMSO, −0.55 V vs SCE in water) which will generate the corresponding semiquinone and diimido species, respectively. The related BQDI complexes[15,16] show similar behavior when they are reduced; the potentials for the Q/Sq and Sq/Cat reductions of **1** are very similar to the unsubstituted BQDI complex and the dimethyl substituted BQDI complex.[16] The oxidation of **1**, however, is quite different from the BQDI complexes which exhibit only a $Ru^{III/II}$ couple, whereas complex **1** has three irreversible oxidation processes. Repeated cycling around the first two processes (between 0.60 and 1.00 V vs SCE) results in the formation of an insulating layer on the electrode surface believed to be caused by the

(45) Balyatinskaya, L. N.; Milyaev, Y. F.; Korshak, A. V. V.; Rusanov, A. L.; Berlin, A. M.; Kereselidze, M. K.; Tabidze, R. S. *J. Gen. Chem. USSR (Engl. Transl.)* **1978**, *48*, 794.

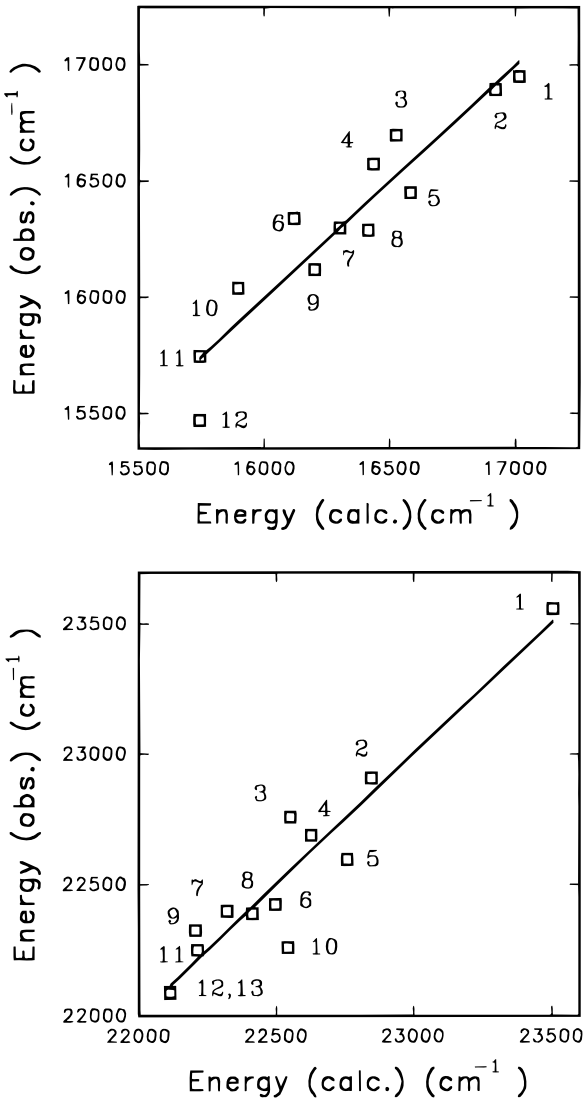

Figure 5. Upper: The correlation of the solvatochromic shift of band I with a combination of the α and β parameters of Kamlet and Taft.[43] (1) Methanol, (2) acetonitrile, (3) propylene carbonate, (4) acetone, (5) ethanol, (6) propan-2-ol, (7) butanol, (8) butanone, (9) tetrahydrofuran, (10) dimethylformamide, (11) dimethylsulfoxide, and (12) dimethylacetamide. Lower: Correlation of the solvatochromic shift of band III with a combination of the α and β parameters of Kamlet and Taft.[43] (1) Water, (2) acetonitrile, (3) acetone, (4) propylene carbonate, (5) methanol, (6) ethanol, (7) butanol, (8) tetrahydrofuran, (9) propan-2-ol, (10) butanone, (11) dimethylformamide, (12) dimethyl sulfoxide, and (13) dimethylacetamide.

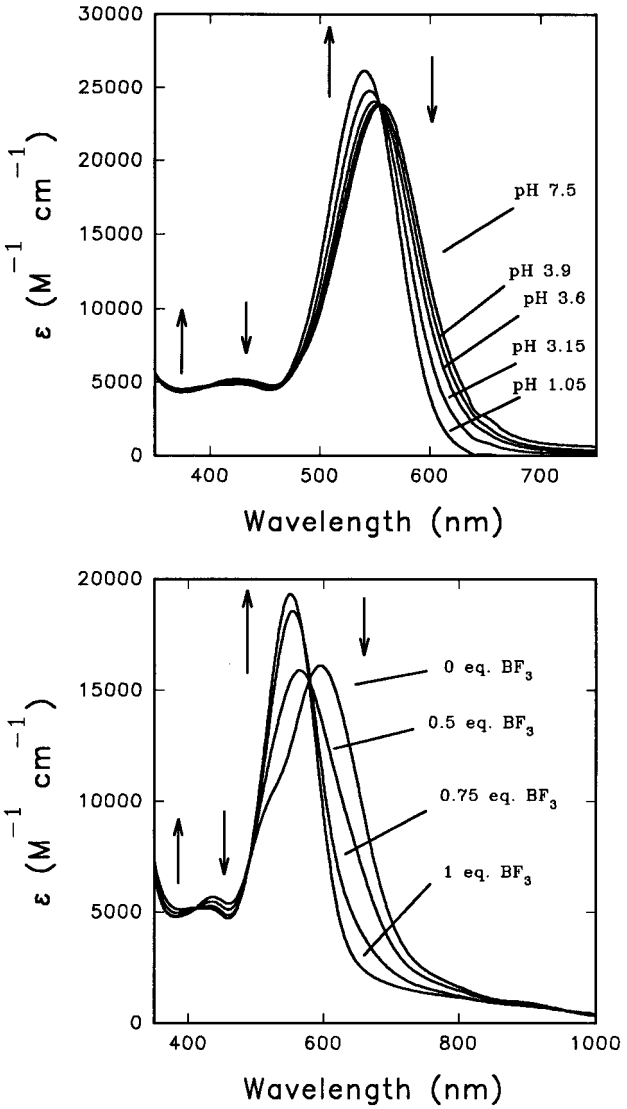

Figure 6. Upper: Spectroscopic shifts that occur as a 2.1×10^{-5} M aqueous solution of the $[Ru(bpy)_2(dadib)](PF_6)_2$ complex is titrated with microliter amounts of 1% or concentrated HCl or 10 M or 0.1 M NaOH with resulting pH as noted. Lower: Spectroscopic changes that occur in the UV−vis spectrum of $[Ru(bpy)_2(dadib)](PF_6)_2$ as equivalents of BF_3 are added, as noted, to a 6.93×10^{-5} M solution of the complex in 1,2-dichloroethane.

oxidation[46] of the ligand amino groups. This potential is too negative to be due to oxidation of the Ru^{II} center. This observation might imply that the HOMO of species **1** is localized on the ligand, but, as will be discussed below, this is not necessarily the case.

The third irreversible process, which occurs at 1.60 V vs SCE is likely oxidation of Ru^{II} occurring at a high potential due to the prior oxidation of the ligand.

3.5. Extended Hückel (EHMO) and Oscillator Strength Calculations, Spectroscopic Assignments, and Mechanism of Donor−Acceptor Coupling. Hydrogen bonding with the imine protons is believed to be responsible for the solvatochromism of the Ru → bpy transition of the "parent" $[Ru(bpy)_2(R_2(BQDI))]^{2+}$ complexes,[15] and shifts of similar, but somewhat higher, magnitude are observed for the Ru → bpy transition in complex **1**. However, with the parent $[Ru(bpy)_2(BQDI)]^{2+}$ species, which must involve solute−solvent interaction at the imino sites, the Ru → π^*(bpy) transition shifts linearly[15] with Gutmann's donor number, DN, in contrast to the dadib situation.

A major difference between the spectroscopy of the dadib system and the parent $[Ru(bpy)_2(BQDI)]^{2+}$ species lies in the importance of charge transfer processes internal to the dadib ligand, i.e. OPDA → BQDI internal charge transfer. The data are best explained by supposing that solvents interact most strongly with the *amino* groups of the OPDA ring of complex **1** modifying the twist angle and the amount of charge injected from the OPDA end to the BQDI end.

In the absence of donors or acceptors, the molecular mechanics minimizer of Spartan 3.0, for the free ligand, placed the 4-amino lone pair in the plane of the ring, hydrogen bonding to a 3-amino hydrogen atom, whereas geometry optimization using the AM1 method for the free ligand or the BF_2^+ complex resulted in both lone pairs being in a position to interact with the π system.

(46) Nemeth, S.; Simandi, L. I.; Argay, G.; Kalmar, A. *Inorg. Chim. Acta* **1989**, *166*, 31.

Table 2. Percentage Ruthenium, OPDA, and BQDI Contribution to Frontier Molecular Orbitals,[a] Using EHMO-CIT Calculations

	coupled, twist angle = 0°			uncoupled, twist angle = 45°		
	%BQDI	%OPDA	%Ru	%BQDI	%OPDA	%Ru
π^*(bpy)[b]	0.2	0.01	4.5	0.2	0.01	4
π^*(bpy)[b]	0.5	0.02	2.0	0.5	0.01	2
LUMO	77	3	16	79	2	17
HOMO	14	19	61	14	1	79
HOMO-1[c]	4	44	47	4	1	83
HOMO-2[c]	5	21	65	0.2	99	1
HOMO-3	19	18	57	20	6	66

[a] Differences of sums of percentages from 100% reflect contribution of wave function located on the bipyridine ligands. Percentages above 0.5% have been rounded to the nearest whole number. [b] In and out of phase combinations of the lowest energy π^* orbitals localized on 2,2′-bipyridine. [c] HOMO-1 and HOMO-2 interchange positions between coupled and uncoupled forms; see text.

EHMO-CIT calculations and transition dipole moment calculations[27] were performed on complex **1** at twist angles (at C2′,C1′,C1,C6) of 0, 30, 45, and 90°, with fixed lone pair configurations. The lone pairs can, in principle, lie in the σ or π plane of the benzene ring. Calculations were carried out for a range of twist angles and lone pair orientations. The experimental data are best reproduced by two models. The data in hydrogen bond acceptor solvents reflect both lone pairs being available for conjugation into the OPDA ring allowing for a donor−acceptor interaction with the ruthenium BQDI ring. This situation was calculated with the lone pairs oriented in the π plane of the OPDA ring (with the 3- and 4-amino lone pairs above and below the OPDA ring to minimize steric hindrance between the NH_2 groups) and with a twist angle of 0°.

The data in hydrogen bond donor solvents reflect the lone pairs being decoupled from the OPDA ring and are calculated assuming a twist angle of 45° with both the lone pairs in the σ plane of the OPDA ring. Similar results are obtained if the lone pairs are retained in the π-plane of OPDA, but the 4-amino or both lone pairs are protonated. We are unable to distinguish spectroscopically which is the more likely configuration.

The dramatic changes in electronic spectra arise because although the electronic transitions occurring in the two extreme cases are basically the same, their oscillator strengths depend critically on the lone pair orientations, i.e., whether the 3- and 4-amino group lone pairs are coupled with the ruthenium BQDI fragment or not. Although the 3-amino group lone pair cannot conjugate directly with the BQDI ring, it can inject charge into the OPDA ring and does influence the oscillator strengths of the various transitions. These oscillator strengths are much less dependent on the actual twist angle chosen. It is reasonable to suppose that with the strong donor−acceptor interaction injecting charge from the π-oriented 4-amino lone pair, the molecule will tend to flatten, while when this interaction is switched off, the H−H repulsion at the 2,6′ and 6,2′ sites will tend to twist the ligand. This was also the conclusion from the earlier AM1 calculations.[1]

In the following discussion, the "coupled" orientation refers to the flat molecule with the 3- and 4-amino group lone pairs coupled into the OPDA ring, while the term "uncoupled" will refer to the converse situation where the lone pairs do not conjugate (because they lie in the σ-plane or because they are protonated) and the ligand dihedral angle is 45°. Key orbitals are displayed in Figure 7 and in Supplementary Information, and their approximate percentage amine, imine, and ruthenium contents, shown in Table 2; note that the difference of their sum from 100% reflects bipyridine orbital content. In this framework, the filled d^6 set will comprise two dπ orbitals with respect to dadib, d_{yz} and d_{xy}, and a dσ orbital ($d_{x^2-z^2}$). The LUMO is largely localized on the ligand BQDI fragment for both lone pair orientations; it is primarily ligand localized but does have some ruthenium d character (dadib π^* − d_{yz}) (ca. 17%) since it is the ligand π^* orbital which is involved in strong coupling through d_{yz} with the metal center (Table 2). The HOMO is mainly a d orbital mixed with a dadib π orbital (d_{xy} − dadib π) which is shared over both rings in the coupled orientation but is almost entirely localized on the BQDI ring in the uncoupled orientation (Table 2).

The HOMO-1, in the coupled molecule, is localized on the metal and the OPDA fragment with significant contributions from both amino group lone pairs. The metal orbital would in fact be a dσ orbital, with respect to dadib lying in the *xz* plane of **1**, in the local RuN_6 microsymmetry. However, because the actual molecule is C_1, this orbital twists (in fact several d orbitals are mixed over HOMO-1 and HOMO-2) and has both σ and π character with respect to the BQDI fragment.

In the uncoupled form HOMO-1 is almost entirely localized on the ruthenium end of the molecule and has much greater d orbital content and some bipyridine π content (Figure 7). The HOMO-1 → LUMO transition is very weak in this form because it is exactly like a $\sigma \rightarrow \pi$ transition, which in the higher local microsymmetry (C_{2v}) would be overlap forbidden. In the lone pair coupled orientation, overlap of HOMO-1 with LUMO is much larger, as is the dipole length, and the oscillator strength of this transition is much larger (see Figure 8). HOMO-2 has substantial ruthenium character (Table 2) in the coupled form, and is σ in character, but also extends over the OPDA fragment (Figure 7). On the other hand, in the uncoupled form, HOMO-2 has essentially no metal character and is localized entirely on the OPDA fragment.

Note that there has in fact been a crossover and the orbital primarily responsible for HOMO-1 in the uncoupled molecule becomes HOMO-2 in the coupled molecule and vice versa; further, it is these two orbitals which share the "dσ" interaction with dadib.

HOMO-3 is the critical bonding orbital (d_{yz} + dadib π^*) between the dπ orbital and the ligand π^* orbital; i.e., it is the bonding counterpart to the LUMO. In the coupled orientation, HOMO-3 spreads over the entire ruthenium dadib fragment, while in the uncoupled form it lies mostly on the ruthenium BQDI fragment with a small amino lone pair contribution.

HOMO-4 is another OPDA localized π orbital which is not shown because we have no experimental evidence for any transition therefrom. However, the HOMO-4 → LUMO transition is calculated to lie between bands II and III and probably contributes to the broadness in this region.

Figure 8 illustrates the stabilization of the d_{yz} orbital below the other ruthenium dπ levels caused by the specific interaction with the dadib π^* LUMO and includes the calculated oscillator strength values. The energy level sequence is similar to those presented for an osmium pyrazine system by Magnuson and Taube[47] and for ruthenium and osmium systems by Creutz and Chou.[48]

The transition dipole moment calculations predict that when the lone pair donation into the ring is maximized (flat molecule), there should be four moderately intense transitions. The most intense (calculated $f = 0.19$) is the HOMO-3 → LUMO transition between the bonding and antibonding combinations of the d_{yz} orbital and the LUMO of the dadib ligand (a $b_2 \rightarrow b_2^*$[15,16] transition in rigorous C_{2v} local symmetry). However, there are two other transitions (excluding the HOMO → LUMO transition to be referred to below) of moderate calculated

(47) Magnuson, R. H.; Taube, H. *J. Am. Chem. Soc.* **1975**, *97*, 5129.
(48) Creutz, C.; Chou, M. H. *Inorg. Chem.* **1987**, *26*, 2995.

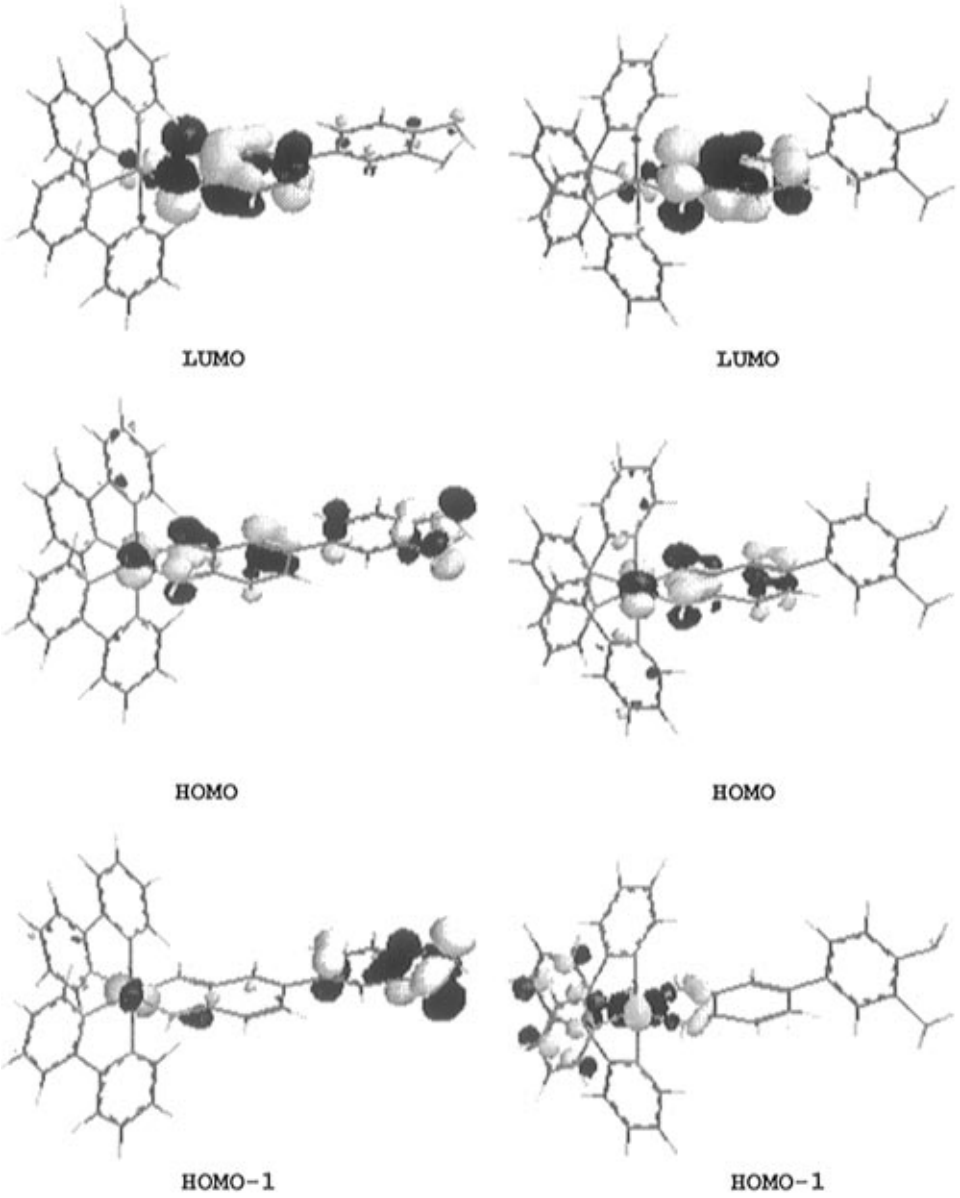

Figure 7. LUMO, HOMO, and HOMO-1 molecular orbital surfaces for complex **1** in the coupled (0° dihedral angle, left) and uncoupled (45° dihedral angle, right) conformations.

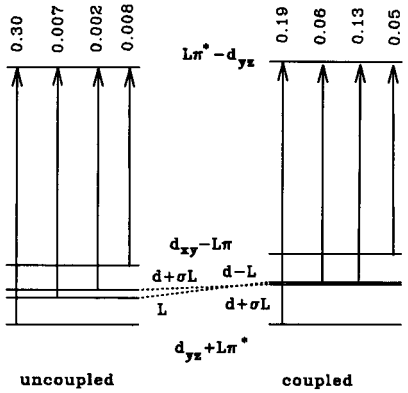

Figure 8. Molecular orbital interaction diagram for the $[Ru(bpy)_2(dadib)](PF_6)_2$ complex, showing EHMO-CIT calculated levels and oscillator strengths in the lone pair uncoupled (45° dihedral angle) and lone pair coupled (0° dihedral angle) situations.

intensity that are predicted to be on the low-energy side of this transition and close in energy (Figure 8) and whose total calculated oscillator strength, $f = 0.19$, is the same as that of the HOMO-3 → LUMO transition.

When the lone pairs are uncoupled from the π system, the HOMO-3 → LUMO transition increases in intensity with a calculated oscillator strength of $f = 0.30$, an almost 2-fold increase in intensity. On the other hand, the two lower energy transitions diminish in intensity with a total oscillator strength now of only 0.009 (Figure 8). The total oscillator strength of all three transitions is seen to be 0.40 and 0.31 in the coupled and uncoupled cases, respectively; i.e., there is little change in the total intensity between the two extremes, and the total calculated value is close to the experimental value of ca. 0.35. While this is very satisfying, one notes that the energies derived from the EHMO-CIT approach are not very good so that the good agreement arises partly from cancellation of errors.

The electronic spectrum of complex **1**, under different conditions, can now be interpreted. The spectrum observed in a hydrogen bond acceptor solvent such as DMSO (lone pair coupled) comprises two transitions (HOMO-1, 2 → LUMO) which probably overlap to produce band I, while the HOMO-3 → LUMO produces band II. Crucially the intensity of the composite band I is predicted to be comparable to that of band II. Band I has significant charge transfer character, both metal

to ligand and internal OPDA to BQDI, consistent with the observation of enhanced internal ligand vibrations in the rR spectra. Band II involves mostly a shift of electron density from ruthenium into the BQDI ring but apparently also some OPDA → BQDI internal charge transfer. This degree of charge transfer seems not to be substantiated by the resonance Raman experiment. Thus, we note that DV−Xα calculations[49] on the first MLCT state of $Cr(CO)_4(bpy)$ reveal very little net electron transfer because of relaxation of the formal $Cr^+(CO)_4(bpy^-)$ state to return charge by donation from bpy^- to Cr^+. Our EHMO-CIT calculation would not take such relaxation into account, if it also occurs here.

In water, or aqueous acid, or with BF_3 in $ClCH_2CH_2Cl$ where the lone pair is uncoupled, band II is also assigned to HOMO-3 → LUMO, but it is expected to be more intense than in the coupled conformation. Band I is not observed since the HOMO-1,2 → LUMO transitions all have very low predicted intensities (10% of that of band II) and may have blue-shifted to lie close to or under band II. The resonance Raman data are consistent with this supposition.

Finally the very weak absorption in the near-infrared (700−1000 nm, see Figures 1, 4, and 6) reasonably corresponds to the HOMO → LUMO transition. This HOMO → LUMO transition is predicted to be moderately intense in the lone pair coupled case with a calculated oscillator strength of 0.05 but becomes much less intense in the uncoupled case ($f = 0.008$). Indeed experimentally this transition is more prominent in DMSO and appears to diminish in aqueous solution or when complex **1** is protonated or coordinates a BF_3 molecule. There are apparently at least two transitions in the near-IR region in water solution, and the higher energy may be HOMO-1 → LUMO.

Note that, in the parent BQDI systems,[15,16] the single intense transition corresponds with HOMO-3 → LUMO in this system, while the weak lower energy absorptions noted in the BQDI system (labeled a_1, a_2 → b_2*) correspond with HOMO and HOMO-1 → LUMO in the uncoupled case, and, hence, their weakness is understood. The calculated and observed oscillator strengths of the principal visible region absorption in the parent $[Ru(bpy)_2(BQDI)]^{2+}$ are 0.28 and 0.26 (in MeCN), respectively.

It is evident that the solid state spectrum (Figure 1) shows both bands I and II, indicative of lone pair donation into the OPDA ring. Thus, intermolecular hydrogen bonding is energetically less important than this intramolecular process.

Table 2 lists the ruthenium contributions to the relevant MOs. Clearly in the lone pair coupled case there is much more Ru d−ligand mixing than in the lone pair uncoupled case, but in both cases the metal−ligand mixing is considerable.

It is now evident that band I is not a single transition but is composite in nature. In the development of eq 3 above, a single transition was presumed. Nevertheless we suppose that the general conclusions are still valid since the peak of band I probably tracks the strongest of these two transitions fairly accurately.

Although the HOMO has extensive d character, this is not inconsistent with the electrochemical experiment which clearly involves oxidation at the ligand. In the spectroscopy, there is no net chemistry, but, in the electrochemical experiment, there is net chemistry with an oxidation product being formed. Amino group oxidation probably leads to a polymerized product, and the difference in free energy of this product from the starting material determines the redox potential. Oxidation probably occurs from HOMO-1 (flat), which has extensive amino lone pair character.

Finally, a note on the EHMO-CI program used herein. Calzaferri[26] has already demonstrated that it is feasible to use EHMO theory to generate oscillator strengths which agree reasonably with experimental data. We have extensively tested[52] our version of this program and have obtained reasonably good agreement with experimental values, at least in the visible and near-IR regions. We do not expect to obtain precise agreement, and the excellent agreement observed here must arise partially due to fortuitous cancellation of errors. We do anticipate that the program is very reliable with respect to trends in oscillator strengths so that distinctions can readily be made between strong, medium, weak, and very weak transitions.

3.6. Ru → bpy Transition and the $Ru^{III/II}$ Redox Potential. The extended Hückel theory does not provide reliable energies, but a combination of the electrochemical data and the optical data can provide an assessment of the relative energies. The energy of band III (Ru → bpy) can be used to calculate the $Ru^{III/II}$ redox potential for this type of complex, according to the following relationship:[50]

$$E(\text{Ru}\rightarrow\text{bpy})/\text{eV} = 0.65E[\text{Ru}^{\text{III/II}}] + 2.00 \qquad (5)$$

Using eq 5 the calculated $Ru^{III/II}$ potential spans the range of 1.14−1.41 V between the extremes of the solvents used. This change of nearly 0.3 V reflects quite a considerable variation in the charge felt by the ruthenium atom passing from water to DMSO and mainly induced by a solute−solvent interaction quite remote from the ruthenium atom (see Table 1).

More cogently, since the reduction potential is largely independent of solvent (see data above), the shift in band I over the solvents studied (experimental value, 0.30 V) should roughly equal the calculated change in the $Ru^{III/II}$ potential as a function of these solvents (Table 1, column 6), namely, 0.27 V. The agreement is very satisfying, especially as variations in the energy of band III are used to predict solvatochromic shifts in band I. Thus, the charge injected into the molecule by the 4-amino lone pair conjugating with the BQDI ring (caused by hydrogen bonding to the NH_2 end) is clearly felt by the ruthenium.

The band II transition energy lies somewhat above that observed (18 200 cm^{-1})[15] in $[Ru(bpy)_2(4,5\text{-}(NH_2)_2BQDI)]^{2+}$ where the two diamino groups are directly attached to the benzoquinonediimine ring. In the previous analysis,[16] a correlation was shown between the Hammett substituent constant of *R* in a series of complexes R_2-BQDI and the $Ru^{III/II}$ potential in the $[Ru(bpy)_2(R_2\text{-BQDI})]^{2+}$ complexes. The dadib ligand may also be considered as a BQDI substituted by the OPDA group. Fitting the dadib data to the previous correlation (Figure 3[16]) allows one to extract a σ_p value[51] for the OPDA ring as −0.59 in the coupled ligand (in DMSO) and +0.18 in the uncoupled ligand (in water).

However, note that with the $[Ru(bpy)_2(R_2\text{-BQDI})]^{2+}$ complexes, a change of substituent with σ_p −0.59 to one with σ_p +0.18 would cause a red shift in the lowest MLCT transition (see Figure 6)[16] but with the dadib system the near-IR band, though not clearly defined, evidently blue shifts for the corresponding change in σ_p

4. Conclusions

Complex **1** has dramatic solvatochromic behavior, which can be explained by a variation of the involvement of the lone pairs

(49) Kobayashi, H.; Kaizu, Y.; Kimura, H.; Matsuzama, H.; Adachi, H. *Mol. Phys.* **1988**, *64*, 1009.
(50) Dodsworth, E. S.; Lever, A. B. P. *Chem. Phys. Lett.* **1986**, *124*, 152.
(51) Hansch, C.; Leo, A.; Taft, R. W. *Chem. Rev.* **1991**, *91*, 165.
(52) DelMedico, A.; Fielder, S. S.; Lever, A. B. P.; Pietro, W. J. Work in progress.

of the amino groups with the OPDA ring and their coupling to the BQDI ring of the dadib ligand. When the lone pairs conjugate with the OPDA ring, the ligand tends toward planarity, while when the lone pairs are decoupled from the OPDA fragment by action of an electron accepting solvent, or by protonation, or by BF_3 coordination, the inter-ring hydrogen−hydrogen repulsions cause the ligand to twist. We have shown through calculation of the oscillator strengths that when the lone pairs inject π electron density into the OPDA ring (flat ligand, hydrogen bond acceptor solvents), there are four transitions of significant intensity. However, with the amino lone pairs decoupled from the OPDA ring (twisted ligand, hydrogen bond donor solvents) only the $d\pi\ b_2 \rightarrow b_2^*$ (π^* LUMO) (labels in C_{2v}, HOMO-3 → LUMO) transition is strong.

The sum of oscillator strengths was shown to be approximately constant for the sum of band I and band II—the latter gains intensity as the former loses intensity with variation in coupling. The agreement between experiment and theory here is striking. It is also striking that band I in the coupled conformation, with an intensity of over 10 000 L mol^{-1} cm^{-1}, arises from the same assignment as the very weak (intensity ca. 100−500 L mol^{-1} cm^{-1}) and easily overlooked bands, observed in the parent $[Ru(bpy)_2(R_2\text{-BQDI})]^{2+}$ series,[16] and related compounds.

The unusual behavior can be understood through symmetry arguments. In the uncoupled version, the effective symmetry of the ruthenium−BQDI fragment approaches C_{2v} in which only the $d\pi\ b_2 \rightarrow b_2\ \pi^*$ LUMO is expected to have significant intensity. The spectrum is then very similar to that of the parent $[Ru(bpy)_2(BQDI)]^{2+}$. In particular the transition from $d_{x^2-z^2}$ (a component of "t_{2g}" in this framework) → π^* LUMO is a $\sigma-\pi$ transition and is strongly overlap forbidden.

In the more planar coupled situation, the effective symmetry must be close to C_1 and all transitions become allowed. In particular the distinction between σ and π is blurred and the transition $d_{x^2-z^2} \rightarrow \pi^*$ LUMO grows dramatically in intensity. The orbital surfaces for the so-called $d_{x^2-z^2}$ orbital (which is a mixed orbital) show that it is tilted out of the $Ru(NH)_2$ plane, explaining how it can then provide a nonzero overlap with the π^* LUMO on the BQDI fragment.

While the EHMO-CIT calculations are usually regarded as relatively crude, the oscillator strengths derived therefrom appear in this case to reproduce the overall features of behavior of this system extraordinarily well. Preliminary ZINDO calculations on this system are in accord with the general conclusions expressed herein.

It is also pleasing that the plots of solvent hydrogen bond donor and acceptor character are fully consistent with the model proposed. One might argue that these plots are prejudiced because band I is actually composite, but the bulk of the intensity does arise from one transition, HOMO-1 → LUMO, so it is probably this transition which is mostly tracked by the solvatochromism analysis.

Magnuson and Taube,[47] considering the osmium−pyrazine system, assumed the splitting between the d_{yz} orbital and the other two (t_{2g}) orbitals, assumed almost nonbonding, was a direct measure of the off-diagonal stabilization of the $d\pi$ orbital caused by π bonding to the pyrazine moiety and was measured approximately by the difference in energy between the MLCT bands which correspond with bands I and II in the osmium−pyrazine system. The principle is the same here, but it is clear that the other $d(t_{2g})$ orbitals are certainly not nonbonding so that the difference in energy between bands I and II is not so readily interpretable. Nevertheless there is evidently considerable mixing between the d_{yz} orbital and the dadib LUMO π^* level. EHMO-CIT calculations show that the LUMO level has 17% ruthenium contribution in both the limiting uncoupled and coupled configurations. This is much larger than the mixing with the bipyridine LUMO π^* level which is calculated to be less than 5%. Indeed we discuss elsewhere[53] the special behavior of the benzoquinonediimine ligand, and related ligands such as the azopyridines, which show dramatic ruthenium d−ligand π^* mixing.

The fact that the coupling between the quinonediimine and the OPDA fragments can be controlled by an external stimulus (solvent) and that this also controls the dihedral angle of the dadib ligand, and the electronic structure of the complex, makes this complex a potential building block for the synthesis of a molecular switching device.

Acknowledgment. We are indebted to the Natural Sciences and Engineering Research Council of Canada (NSERC, Ottawa) and the Office of Naval Research (Washington, D. C.) for financial support and the Johnson Matthey Co. for the loan of ruthenium trichloride. We would also like to thank Theo L. Snoeck for measuring the rR spectra, Dr. Hitoshi Masui for valuable discussion, and Lori Payne for technical support.

Supporting Information Available: Figures of molecular orbital pictures for the HOMO-2 and HOMO-3 in the coupled (0° dihedral angle) and uncoupled conformations (45° dihedral angle) (2 pages). Ordering information is given on any current masthead page.

IC960232S

(53) Vlcek, A. A.; Fielder, S. S.; Pietro, W. J.; Lever, A. B. P. Submitted for publication in *Inorg. Chem*. Dodsworth, E. S.; Gorelsky, S. I.; Lever, A. B. P. Manuscript in preparation.